Higher-order mode suppression in chalcogenide negative curvature fibers

Chengli Wei,[1] Robinson A. Kuis,[2] Francois Chenard,[3] Curtis R. Menyuk,[2] and Jonathan Hu[1,*]

[1]*Baylor University, One Bear Place #97356, Waco, TX 76798 USA*
[2]*University of Maryland Baltimore County, 5200 Westland Blvd., Baltimore, MD 21227 USA*
[3]*IRflex Corporation, 300 Ringgold Industrial Parkway, Danville, VA 24540 USA*

[*] *Jonathan_hu@baylor.edu*

Abstract: We find conditions for suppression of higher-order core modes in chalcogenide negative curvature fibers with an air core. An avoided crossing between the higher-order core modes and the fundamental modes in the tubes surrounding the core can be used to resonantly couple these modes, so that the higher-order core modes become lossy. In the parameter range of the avoided crossing, the higher-order core modes become hybrid modes that reside partly in the core and partly in the tubes. The loss ratio of the higher-order core modes to the fundamental core mode can be more than 50, while the leakage loss of the fundamental core mode is under 0.4 dB/m. We show that this loss ratio is almost unchanged when the core diameter changes and so will remain large in the presence of fluctuations that are due to the fiber drawing process.

OCIS codes: (060.2280) Fiber design and fabrication; (060.2400) Fiber properties; (060.2390) Fiber optics, infrared.

References and links

1. J. Broeng, S. E. Barkou, T. Søndergaard, and A. Bjarklev, "Analysis of air-guiding photonic bandgap fibers," Opt. Lett. **25**(2), 96–98 (2000).
2. G. Pearce, J. Pottage, D. Bird, P. Roberts, J. Knight, and P. Russell, "Hollow-core PCF for guidance in the mid to far infra-red," Opt. Express **13**(18), 6937–6946 (2005).
3. J. Hu and C. R. Menyuk, "Leakage loss and bandgap analysis in air-core photonic bandgap fiber for nonsilica glasses," Opt. Express **15**(2), 339–349 (2007).
4. P. Russell, "Photonic-Crystal Fibers," J. Lightwave Technol. **24**(12), 4729–4749 (2006).
5. J. C. Knight, J. Broeng, T. A. Birks, and P. S. J. Russell, "Photonic band gap guidance in optical fibers," Science **282**(5393), 1476–1478 (1998).
6. F. Yu and J. C. Knight, "Spectral attenuation limits of silica hollow core negative curvature fiber," Opt. Express **21**(18), 21466–21471 (2013).
7. F. Yu, W. J. Wadsworth, and J. C. Knight, "Low loss silica hollow core fibers for 3–4 μm spectral region," Opt. Express **20**(10), 11153–11158 (2012).
8. W. Belardi and J. C. Knight, "Effect of core boundary curvature on the confinement losses of hollow antiresonant fibers," Opt. Express **21**(19), 21912–21917 (2013).
9. P. Jaworski, F. Yu, R. R. J. Maier, W. J. Wadsworth, J. C. Knight, J. D. Shephard and D. P. Hand, "Picosecond and nanosecond pulse delivery through a hollow-core negative curvature fiber for micro-machining applications," Opt. Express **21**(19), 22742–22753 (2013).
10. A. D. Pryamikov, A. S. Biriukov, A. F. Kosolapov, V. G. Plotnichenko, S. L. Semjonov, and E. M. Dianov, "Demonstration of a waveguide regime for a silica hollow-core microstructured optical fiber with a negative curvature of the core boundary in the spectral region > 3.5 μm," Opt. Express **19**(2), 1441–1448 (2011).
11. W. Belardi and J. C. Knight, "Hollow antiresonant fibers with reduced attenuation," Opt. Lett. **39**(7), 1853–1856 (2014).

#235805 - $15.00 USD Received 23 Mar 2015; revised 11 May 2015; accepted 17 May 2015; published 8 Jun 2015

12. W. Belardi and J. C. Knight, "Hollow antiresonant fibers with low bending loss," Opt. Express **22**(8), 10091–10096 (2014).
13. F. Poletti, "Nested antiresonant nodeless hollow core fiber," Opt. Express **22**(20), 23807–23828 (2014).
14. A. F. Kosolapov, A. D. Pryamikov, A. S. Biriukov, V. S. Shiryaev, M. S. Astapovich, G. E. Snopatin, V. G. Plotnichenko, M. F. Churbanov, and E. M. Dianov, "Demonstration of CO_2-laser power delivery through chalcogenide-glass fiber with negative-curvature hollow core," Opt. Express **19**(25), 25723–25728 (2011).
15. V. S. Shiryaev, A. F. Kosolapov, A. D. Pryamikov, G. E. Snopatin, M. F. Churbanov, A. S. Biriukov, T. V. Kotereva, S. V. Mishinov, G. K. Alagashev, A. N. Kolyadin, "Development of technique for preparation of As_2S_3 glass preforms for hollow core microstructured optical fibers," J. Optoelectron. Adv. M. **16**(9–10), 1020–1025 (2014).
16. L. Vincetti and V. Setti, "Waveguiding mechanism in tube lattice fibers," Opt. Express **18**(22), 23133–23146 (2010).
17. L. B. Fu, M. Rochette, V. G. Ta'eed, D. J. Moss, and B. J. Eggleton, "Investigation of self-phase modulation based optical regenerator in single mode As_2Se_3 chalcogenide glass fiber," Opt. Express **13**(19), 7637–7644 (2005).
18. J. S. Sanghera, L. Brandon Shaw, and I. D. Aggarwal, "Chalcogenide glass-fiber-based mid-IR sources and applications," IEEE J. Sel. Top. Quantum Electron. **15**(1), 114–119 (2009).
19. B. Debord, M. Alharbi, T. Bradley, C. Fourcade-Dutin, Y. Y. Wang, L. Vincetti, F. Gérôme, and F. Benabid, "Hypocycloid-shaped hollow-core photonic crystal fiber Part I: Arc curvature effect on confinement loss," Opt. Express **21**(23), 28597–28608 (2013).
20. J. M. Fini, "Aircore microstructure fibers with suppressed higher-order modes," Opt. Express **14**(23), 11354–11361 (2006).
21. K. Saitoh, N. J. Florous, T. Murao, and M. Koshiba, "Design of photonic band gap fibers with suppressed higher-order modes: Towards the development of effectively single mode large hollow-core fiber platforms," Opt. Express **14**(16), 7342–7352 (2006).
22. J. M. Fini, J. W. Nicholson, R. S. Windeler, E. M. Monberg, L. Meng, B. Mangan, A. Desantolo, and F. V. DiMarcello, "Low-loss hollow-core fibers with improved single-modedness," Opt. Express **21**(15), 6233–6242 (2013).
23. T. Murao, K. Saitoh and M. Koshiba, "Multiple resonant coupling mechanism for suppression of higher-order modes in all-solid photonic bandgap fibers with heterostructured cladding," Opt. Express **19**(3), 1713–1727 (2011).
24. F. Jansen, F. Stutzki, C. Jauregui, J. Limpert, and A. Tünnermann, "Avoided crossings in photonic crystal fibers," Opt. Express **19**(14), 13578–13589 (2011).
25. J. A. West, C. M. Smith, N. F. Borrelli, D. C. Allan, and K. W. Koch, "Surface modes in air-core photonic band-gap fibers," Opt. Express **12**(8), 1485–1496 (2004).
26. K. Saitoh and M. Koshiba, "Leakage loss and group velocity dispersion in air-core photonic bandgap fibers," Opt. Express **11**(23), 3100–3109 (2003).
27. T. P. White, B. T. Kuhlmey, R. C. McPhedran, D. Maystre, G. Renversez, C. M. de Sterke and L. C. Botten, "Multipole method for microstructured optical fibers. I. Formulation," J. Opt. Soc. Am. B **19**(10), 2322–2330 (2002).
28. G. Ren, Z. Wang, S. Lou, and S. Jian, "Mode classification and degeneracy in photonic crystal fibers," Opt. Express **11**(11), 1310–1321 (2003).
29. J. Hu, C. R. Menyuk, L. B. Shaw, J. S. Sanghera, and I. D. Aggarwal, "Computational study of a 3–5 μm source that is created by using supercontinuum generation in As_2S_3 chalcogenide fibers with a pump at 2 μm," Opt. Lett. **35**(17), 2907–2909 (2010).
30. N. M. Litchinitser, A. K. Abeeluck, C. Headley, and B. J. Eggleton, "Antiresonant reflecting photonic crystal optical waveguides," Opt. Lett. **27**(18), 1592–1594 (2002).
31. N. M. Litchinitser, S. C. Dunn, B. Usner, B. J. Eggleton, T. P. White, R. C. McPhedran, and C. M. de Sterke, "Resonances in microstructured optical waveguides," Opt. Express **11**(10), 1243–1251 (2003).
32. G. Renversez, P. Boyer, and A. Sagrini, "Antiresonant reflecting optical waveguide microstructured fibers revisited: a new analysis based on leaky mode coupling," Opt. Express **14**(12), 5682–5687 (2006).
33. F. Gérôme, R. Jamier, J. L. Auguste, G. Humbert, and J. M. Blondy, "Simplified hollow-core photonic crystal fiber," Opt. Lett. **35**(8), 1157–1159 (2010).
34. P. K. Choudhury and T. Yoshino, "A rigorous analysis of the power distribution in plastic clad annular core optical fibers," Optik **113**(111), 481–488 (2002).
35. M. Hautakorpi and M. Kaivola, "Modal analysis of M-type-dielectric-profile optical fibers in the weakly guiding approximation," J. Opt. Soc. Am. A **22**(6), 1163–1169 (2005).
36. W. Ding and Y. Wang, "Analytic model for light guidance in single-wall hollow-core anti-resonant fibers," Opt. Express **22**(22), 27242–27256 (2014).

#235805 - $15.00 USD Received 23 Mar 2015; revised 11 May 2015; accepted 17 May 2015; published 8 Jun 2015

1. Introduction

Hollow-core photonic crystal fibers (PCFs) confine the light inside a hollow air core that is surrounded by a microstructured glass cladding [1–5]. These hollow-core PCFs have the potential to provide low-loss transmission, along with delivery of high-power light with low nonlinearity. The oldest and most common approach for confining light in the core is to use a photonic bandgap structure in the cladding that is created by a periodic array of air holes [3–5]. Light cannot propagate in the cladding in the wavelength range of the bandgap and is confined within the hollow core. An alternative approach that has recently been investigated is to use negative curvature at the core-cladding boundary by placing a set of hollow tubes that surround the hollow core [6–16]. Negative curvature implies that the surface normal to the core boundary is oppositely directed from the core [6, 7]. Since no bandgap is used, there is no requirement for a periodic cladding structure. Chalcogenide fibers are often used for infrared transmission at wavelengths beyond 3 μm where silica fibers become lossy [17, 18]. However, development of hollow-core chalcogenide fibers has been hampered by fabrication difficulties. Negative curvature fibers have a simpler structure than photonic bandgap fibers, which makes it easier in principle to fabricate them.

Negative curvature fibers have been simulated and fabricated in silica with core diameters ranging from 30 μm to 110 μm for transmission wavelengths between 1 μm and 4 μm [6–13]. A chalcogenide negative curvature fiber has been fabricated with a large core size of 380 μm to transmit light from a CO_2 laser at 10.6 μm [14]. Fibers with a large core diameter like this one have low-loss transmission with low nonlinearity. On the other hand, fibers with a large core diameter have higher-order core modes. It is desirable for many applications to suppress the higher-order modes, which would decrease the coupling between the fundamental and higher-order core modes due to small perturbations like microbending [19, 20].

In this paper, we show computationally that it is possible to suppress higher-order core modes in a chalcogenide negative curvature fiber while preserving low leakage loss for the fundamental core mode. The mechanism is resonant coupling between the higher-order core modes and the fundamental tube modes. This approach is analogous to using defect modes in a photonic bandgap fiber [20–23]; however, there is no need to create defects in this case, since the tubes that create the negative curvature can also provide the resonant coupling. Avoided crossings lead to high loss for fiber modes [24, 25]. It is possible to design negative curvature fiber so that an avoided crossing between the higher-order core modes and the fundamental tube modes leads to an increase in the loss of the higher-order core modes. The higher-order core modes in the parameter range of the avoided crossing are really hybrid modes that reside partly in the core and partly in the tubes. The loss ratio of the higher-order core modes to the fundamental core mode can be greater than 50, while the leakage loss for the fundamental core mode is still under 0.4 dB/m.

2. Fiber geometry

We calculate the fiber modes and their propagation constants using Comsol Multiphysics, a commercial full-vector mode solver based on the finite-element method. Anisotropic, perfectly matched layers (PMLs) are positioned outside the cladding in order to reduce the size of the simulation window [26]. Figure 1 shows the full hollow-core PCF geometry. The gray regions represent glass, and the white regions represent air. Only a quarter of the geometry is used in modeling hollow-core PCFs because of the symmetry of the modes [27, 28]. We model a hollow-core PCF with eight cladding tubes. The inner tube diameter, d_{tube}, and the inner core diameter D_{core}, are related by the expression $D_{\text{core}} = (d_{\text{tube}} + 2t)/\sin(\pi/8) - (d_{\text{tube}} + 2t)$. We use t to denote the thickness of the tube walls. We use a core diameter, $D_{\text{core}} = 60$ μm, and a wavelength, $\lambda = 2$ μm. We vary the tube wall thickness t to obtain an avoided crossing. We

#235805 - $15.00 USD Received 23 Mar 2015; revised 11 May 2015; accepted 17 May 2015; published 8 Jun 2015

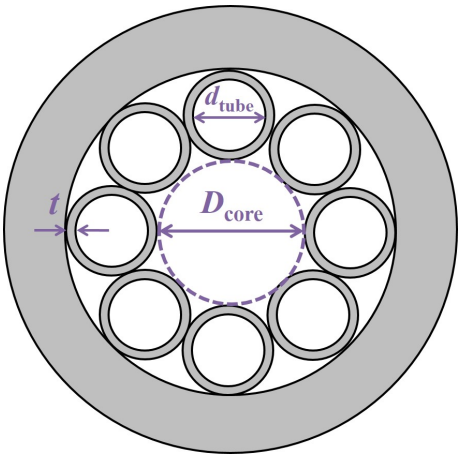

Fig. 1. Cross-section of the chalcogenide negative curvature fiber.

simulate As_2S_3 chalcogenide glass with a refractive index whose real part equals 2.4 and whose imaginary part equals 1.1×10^{-8} [29].

3. Avoided crossing between higher-order core modes and tube modes

In order to confine light in the core of the negative curvature fiber, the wall thickness of the tubes must not be resonant with the wavelength of the light. Resonance occurs when $t = m\lambda/[2(n_1^2 - n_0^2)^{1/2}]$, where m is any positive integer, λ is the light wavelength, and where $n_1 = 2.4$ and $n_0 = 1.0$ are the real parts of the refractive indices of chalcogenide glass and air, respectively. At resonance, the phase of the electric field changes by a multiple of 2π from one side of the tube wall to the other [30–33]. The values of t that correspond to $m = 1$, 2, and 3 are 0.46, 0.92, and 1.38 μm, respectively. We study the first transmission band, so that $t < 0.46$ μm. Figure 2(a) shows the real part of the effective indices of the core modes and the tube modes as a function of t. Figure 2(b) shows the loss of the core modes, and Fig. 2(c) shows the ratio of the loss of the TE_{01} to the loss of the HE_{11} core mode. The TE_{01} mode is the higher-order core mode that has the lowest loss, and the HE_{11} mode is the fundamental core mode. The loss ratio of these two modes reaches a maximum of 58 when $t = 0.42$ μm; at this wall thickness, the loss of the fundamental core mode is 0.32 dB/m. Hence, higher-order core modes can be suppressed in combination with low transmission loss for the fundamental core mode.

We repeated the same analysis for the second and third transmission bands. The maximum loss ratio of the higher-order core modes to the fundamental core mode reaches 39 and 28 when $t = 0.88$ and 1.33 μm, respectively. The corresponding losses of the fundamental core modes are 0.4 and 0.55 dB/m.

In order to study the coupling mechanism, we show the avoided crossing between the TE_{01} core mode and the corresponding tube mode that couples to it at the avoided crossing. In Figs. 3–5, we use A1, A2, and A3 to label the fundamental core mode (HE_{11} mode) when $t = 0.32$, 0.42, and 0.44 μm, respectively. We use B1, B2, and B3 to label the TE_{01} core mode and C1, C2, and C3 to label the corresponding tube mode at the same three thicknesses. Figure 3(a) shows the real part of the effective index for the TE_{01} core mode and the corresponding tube mode as the tube thickness increases from 0.32 to 0.44 μm. For reference, we also show the real part of the effective index of the fundamental core mode. Since both the TE_{01} core mode and the corresponding tube mode reside in air and interact with the same tube wall, they

#235805 - $15.00 USD Received 23 Mar 2015; revised 11 May 2015; accepted 17 May 2015; published 8 Jun 2015

vary in a similar way as the wall thickness increases. As a consequence, the avoided crossing happens slowly as the tube thickness changes from 0.40 to 0.44 μm. Nonetheless, the avoided crossing is clearly visible in the effective index and in the mode fields. The difference of the effective indices between the TE_{01} core mode and the corresponding tube mode, as shown in Fig. 3(b), reaches a minimum at $t = 0.42$ μm, which is also the tube thickness at which the loss ratio of the TE_{01} core mode to the fundamental HE_{11} core mode reaches its maximum, as shown in Fig. 2(c).

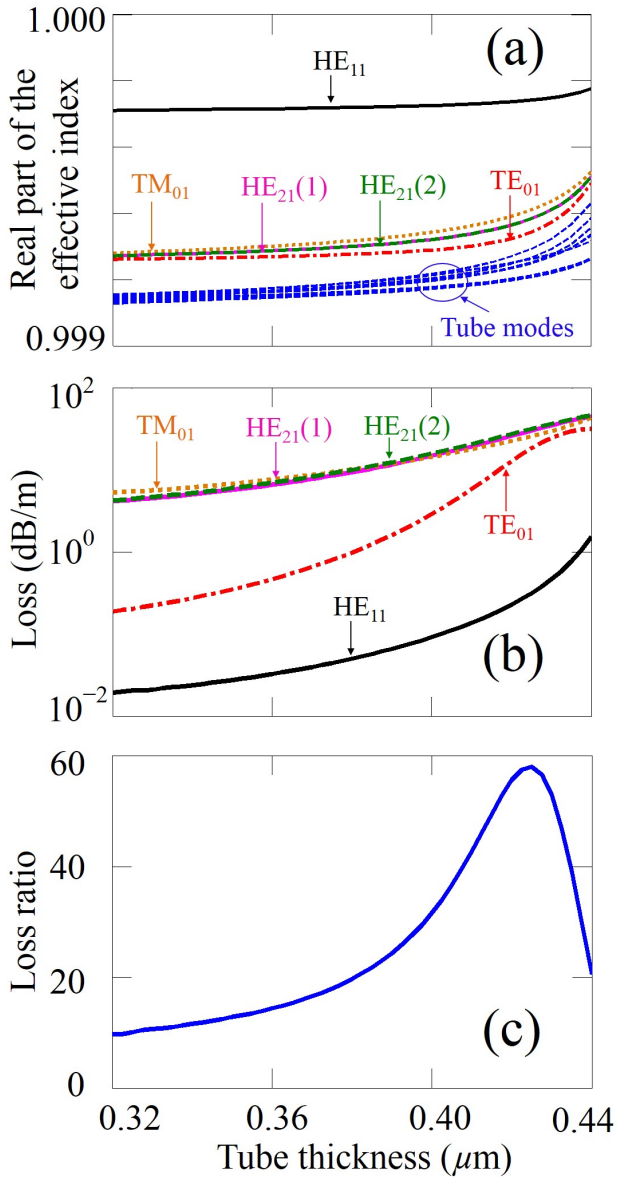

Fig. 2. Real part of (a) the effective index and (b) the leakage loss of the fundamental HE_{11} core mode, the TE_{01} core mode, the TM_{01} core mode, and the two degenerate HE_{21} core modes in the chalcogenide negative curvature fiber. The blue dashed curves correspond to the tube modes. (c) Loss ratio of the TE_{01}core mode to the fundamental HE_{11} core mode.

#235805 - $15.00 USD Received 23 Mar 2015; revised 11 May 2015; accepted 17 May 2015; published 8 Jun 2015

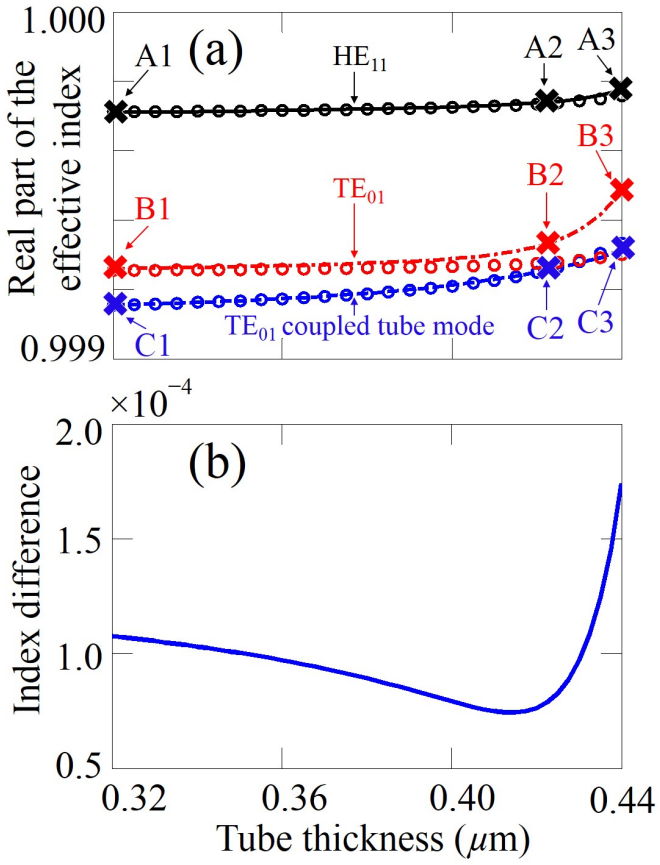

Fig. 3. (a) Real part of the effective index of the HE_{11} core mode, the TE_{01} core mode and corresponding tube mode that couples to the TE_{01} core mode. The open circles represent the real part of the effective index of the corresponding modes using the annular core fiber model. (b) Effective index difference between the TE_{01} core mode and tube mode that is coupled to the TE_{01} core mode.

We show the mode fields in Fig. 4. The color indicates the electric field, normalized to its maximum, while the arrows indicate the direction of the transverse electric field and the lengths of the arrows are propotional to the amplitude of the transverse electric field. When $t = 0.32$ μm, both the TE_{01} core mode and the corresponding tube mode are well-confined to the core and the tubes, respectively. When $t = 0.42$ μm, in the center of the parameter range in which the avoided crossing occurs, both the original TE_{01} core mode and corresponding tube mode reside partly in the core and partly in the cladding tubes. Both have effectively become hybrid modes. When $t = 0.44$ μm, most of the original TE_{01} core mode resides in the tubes and vice versa. In Fig. 5, we show the ratios of the power in the core and the power in the tubes to the total power in the fiber for both modes as a function of t. The crossing point, which occurs at $t = 0.43$ μm, is clearly visible. By contrast, the fundamental core mode is almost unaffected by the avoided crossing, and the fraction of its power that is in the core falls gradually from 0.98 to 0.88 as t increases from 0.32 μm to 0.44 μm. Note that other higher-order core modes, the TM_{01} and HE_{21} modes also have avoided crossings at $t = 0.42$ μm, although the effect of the avoided crossing is not as strong as the effect on the TE_{01} core mode, as shown in Fig. 2(b).

#235805 - $15.00 USD Received 23 Mar 2015; revised 11 May 2015; accepted 17 May 2015; published 8 Jun 2015

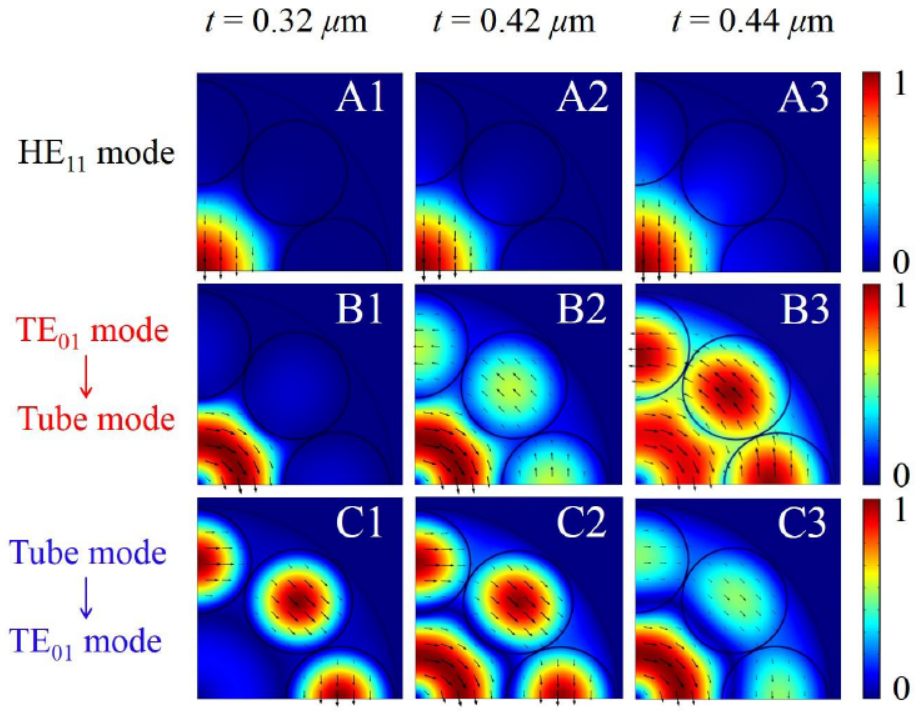

Fig. 4. Mode fields of the HE_{11} core mode, the TE_{01} core mode, and the tube mode that couples with the TE_{01} core mode at tube thicknesses of 0.32 μm, 0.42 μm and 0.44 μm, respectively, corresponding to the labeled crosses in Fig. 3(a) and Fig. 5. The contour plots represent the normalized electric field intensity and the arrows represent the amplitude and direction of the transverse electric field.

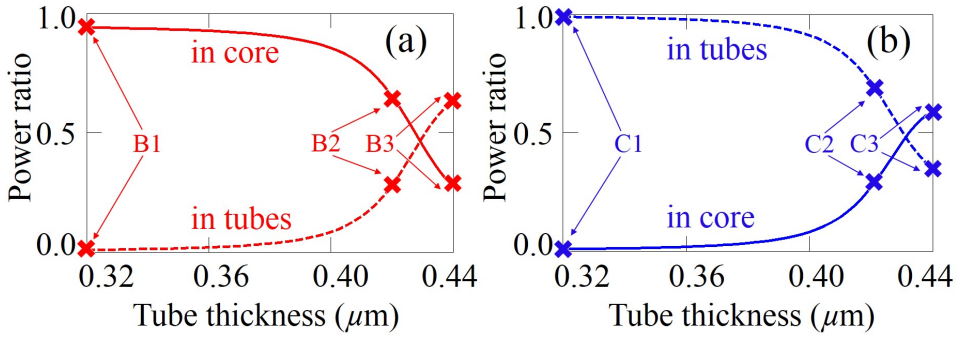

Fig. 5. (a) The power ratio in the core and the power ratio in the tubes for the TE_{01} core mode. (b) The power ratio in the core and the power ratio in the tubes for the corresponding tube mode that couples with the TE_{01} core mode.

#235805 - $15.00 USD Received 23 Mar 2015; revised 11 May 2015; accepted 17 May 2015; published 8 Jun 2015

4. Comparison between negative curvature fibers and annular core fibers

Here, we analyze the higher-order core modes and fundamental tube modes in a negative curvature fiber when they are effectively decoupled, which allows us to predict when an avoided crossing will occur. We use annular core fibers to predict the effective indices of the modes in the air core and a cladding tube of a negative curvature fiber. The annular core fiber is just a glass ring suspended in air [34–36]. Figure 6 shows two different annular core fibers used to study the modes in the core and a cladding tube of the negative curvature fiber. To study the modes in the tube, we use an annular core fiber with the same glass thickness and core diameter as the tubes in the negative curvature fiber. To study the modes in the air core, we use an annular core fiber with the same glass thickness as the glass thickness in the negative curvature fiber. We increase the core diameter in the annular core fiber by 5% to account for the effective increase in the core diameter that occurs in a negative curvature fiber. With this increase in the core diameter, we have found that the effective indices of the core modes in the negative curvature fiber match the effective indices of the modes in the corresponding annular core fiber within 0.001% for the tube thicknesses between 0.32 and 0.37 μm, as shown in Fig. 3(a). We solve for the modes in the air core of the annular core fiber and plot the real part of the effective indices of different modes as open circles in Fig. 3(a). The blue circles represent the effective index of the tube mode using an annular core fiber with the same diameter as a single tube in the negative curvature fiber. The black and red circles represent the effective indices of the fundamental core mode and the TE_{01} core mode, respectively. We can see that corresponding solid curves and circles agree very well for tube thicknesses between 0.32 and 0.37 μm. At a larger tube thickness region, the blue circles and red circles cross each other at the tube thickness of the 0.42 μm. Hence, the crossing point of the decoupled modes in the annular core fibers is consistent with the avoided-crossing point of the coupled modes in the negative curvature fiber, as shown in Section 3. Annular core fibers can thus be used to provide a simple prediction of the avoided crossing between the higher-order core modes and the tube modes.

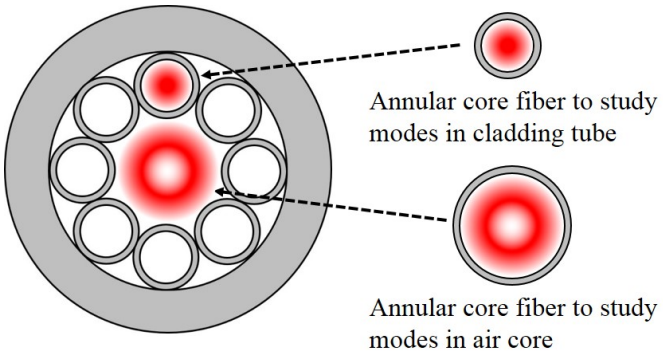

Fig. 6. Annular core fibers are used to study the modes in the tube and the core of a negative curvature fiber.

5. Higher-order mode suppression with different core diameters

We also studied the possibility of suppressing higher-order core modes by using different core diameters or a different number of tubes. When we increase the core diameter, we increase the tube diameter proportionally. The effective indices of the modes in the core and tubes change by nearly the same amount. We find that the index difference between the higher-order (TE_{01}) core mode and the corresponding coupled tube modes only changes by 2×10^{-5} when the core diameter changes from 50 μm to 60 μm. Hence, changing the core diameter does not significantly

#235805 - $15.00 USD Received 23 Mar 2015; revised 11 May 2015; accepted 17 May 2015; published 8 Jun 2015

change the resonant coupling condition. On the other hand, one can benefit from this property because as one varies the core diameter, the avoided crossing condition and the higher-order mode suppression still occur. In addition, the loss of the fundamental core mode decreases as the core diameter increases. Figure 7 shows the loss coefficient of the fundamental core mode as a red solid curve, and it shows the loss ratio of the lowest-loss, higer-order (TE_{01}) core mode relative to the fundamental core mode as a blue dashed curve, as one changes core diameter. The tube thickness is fixed at 0.42 μm. The loss of the fundamental core mode decreases from 0.38 to 0.27 dB/m, while the loss ratio varies between 55 and 59 when we increase the core diameter from 58 to 62 μm. Hence, the higher-order mode suppression will be robust in the presence of core diameter fluctuations due to the fiber drawing process.

Instead of increasing the diameter of the tubes, one might increase the number of tubes, in which case the core diameter does not change and the tube diameter decreases. At the end, the effective index for the core mode does not change much and the effective index for the cladding tube mode decreases. The increasing index difference between the higher-order core modes and cladding tube modes will not enable resonant coupling between the higher-order core modes and cladding tube modes. On the other hand, if we decrease the number of tubes from eight to six, the hexagonal fiber structure would effectively have the same core diameter and tube diameter. In this case, the fundamental core mode would easily couple to the tube modes, which should be avoided.

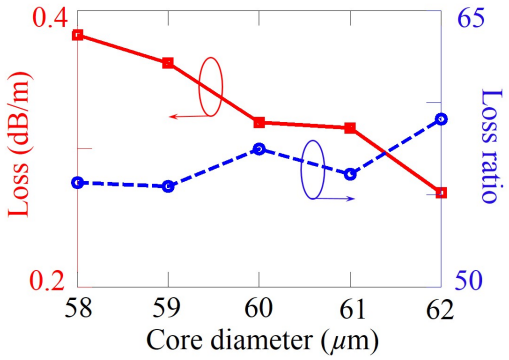

Fig. 7. Loss of the fundamental core mode and loss ratio of the lowest-loss, higer-order (TE_{01}) core mode to the fundamental core mode as a function of core diameter. The tube thickness is fixed at 0.42 μm.

6. Conclusion

In this paper, we study higher-order core mode suppression in chalcogenide negative curvature fibers. In a negative curvature fiber, there is no need to create additional defect cores in the cladding region. The cladding tubes automatically serve as outer defect cores. The higher-order core modes can be suppressed using the avoided crossing between the higher-order core modes and the corresponding cladding tube modes. When the core diameter is 60 μm and the tube thickness is 0.42 μm, the loss ratio of the higher-order core modes to the fundamental core mode can be more than 50, while the leakage loss of the fundamental core mode is still under 0.4 dB/m. The higher-order core mode suppression is robust even with fluctuations of the core diameter that are induced by the fiber drawing process.

Acknowledgments

This research was supported in part by funds from the Vice Provost for Research at Baylor University.

#235805 - $15.00 USD Received 23 Mar 2015; revised 11 May 2015; accepted 17 May 2015; published 8 Jun 2015